



## Revista Internacional de Investigación e Innovación Tecnológica

Página principal: [www.riit.com.mx](http://www.riit.com.mx)

### **Mechanical properties assessment of a high strength automotive steel processed via Quenching and Partitioning**

### **Evaluación de las propiedades mecánicas de un acero automotriz de alta resistencia procesado via Quenching and Partitioning**

**Sias-Chacón, A.<sup>a</sup>, Covarrubias-Alvarado, O.<sup>b</sup>, Pérez-Unzueta, A.<sup>b</sup>**

<sup>a</sup> Department of Ferrous Metallurgy, RWTH Aachen University, Intzestr1, 52072 Aachen, Germany.

<sup>b</sup> Department of Materials Engineering, Universidad Autónoma de Nuevo León, Pedro de Alba S/N, San Nicolás de los Garza, N.L., México.

[sias.arisbeth@hotmail.es](mailto:sias.arisbeth@hotmail.es); [novenius@gmail.com](mailto:novenius@gmail.com); [betinperez@hotmail.com](mailto:betinperez@hotmail.com)

**Technological innovation:** Development of heat treatments for automotive steels.

**Area of application:** Automotive industry.

Received: Jul 01th, 2019

Accepted: December 20th, 2019

### **Resumen**

La industria automotriz se ha enfocado en la fabricación de vehículos más ligeros, lo que ha llevado a un aumento del uso de componentes de acero estampados en caliente. Sin embargo, la mejora de la formabilidad sigue siendo un desafío para estos aceros. El nuevo proceso de Quenching and Partitioning (Q&P) ofrece una buena alternativa para producir aceros con alta resistencia y al mismo tiempo formables, basándose en el desarrollo de una microestructura compuesta de martensita y austenita retenida.

El objetivo de esta investigación es mejorar la formabilidad manteniendo una alta resistencia mecánica, utilizando la microestructura resultante de los tratamientos Q&P para un acero comercial CSiMn. El acero investigado se austenitizó totalmente, posteriormente fue templado a una temperatura inferior a la temperatura de inicio de la formación de martensita ( $M_s$ ), seguido de una retención isotérmica a la misma temperatura (un paso) y a una temperatura más elevada (dos pasos). La formabilidad se caracterizó, por una parte, en términos de la elongación uniforme y la elongación total, determinadas por medio de pruebas de tracción y, por otra parte, utilizando el ángulo de flexión máximo alcanzable mediante ensayos de flexión a tres puntos. Los resultados

indicaron que la formabilidad es mayor con partición a 440 °C durante 100 segundos, lo que sugiere un fuerte efecto a la plasticidad inducida por transformación (TRIP, por sus siglas en inglés) debido a fracciones mayores de austenita estable. Mientras que, a temperaturas de partición más bajas, las cantidades menores de austenita retenida y la baja capacidad de formado resultantes pueden explicarse por la precipitación de carburos que suprimen la estabilización de la austenita retenida.

**Palabras clave:** Ductilidad, Alta resistencia, Martensita, Particionado, Austenita retenida.

## Abstract

The emphasis of the automotive industry in manufacturing vehicles of reduced weight has led to an increase in the usage of hot stamped steel components. However, improving the formability is still a challenge for these steels. The new Quenching and Partitioning (Q&P) process offers a good alternative to produce high strength and at the same time, formable steels based on the development of a microstructure consisting of martensite and retained austenite.

This research is focused on the enhancement of formability while maintaining a high mechanical strength using the feature of the microstructure developed after Q&P treatments for a commercially produced CSiMn steel. The investigated steel was fully austenitized with subsequent quenching to a temperature below the martensite start temperature ( $M_s$ ), followed by isothermal holding at the same temperature (one-step) and by reheating to higher temperature (two-step). Formability was on the one hand characterized by using the common description in terms of uniform and total elongation from tensile tests and on the other hand, by using a maximum achievable bending angle determined from three-point bending tests. The outcomes indicated that the enhancement of the formability is higher with partitioning at 440 °C for 100 seconds, suggesting a strong Transformation Induced Plasticity (TRIP) effect due to larger fractions of stable austenite. Whereas at lower partitioning temperatures the reduced amounts of retained austenite and the consequently lower formability can be explained by carbides precipitation which suppress the stabilization of retained austenite.

**Key words:** Ductility, High strength, Martensite, Partitioning, Retained austenite.

## 1. Introduction

The need to simultaneously reduce the weight of vehicles and increase crash worthiness for safety requires the use of thinner and higher strength steels with improved formability. The hot stamping technology is one of the most effective methods to produce high strength steels for car components. The hot stamping is a non-isothermal process designed for sheet metals, in which forming and quenching take place at the same forming stage [1]. Its main advantage is the excellent

shape accuracy of the components, allowing the use of thinner gauge sheet metal. Therefore, weight reduction can be achieved while maintains structural integrity, by enabling the production of high strength parts without problems with cracking or springback and the achievement of a high tensile strength of approximately 1500 MPa [2]. Nevertheless, the requirement of a high strength has led to concerns about the in-service properties such as ductility, residual bendability, and fatigue.

In the context of automotive structures, the so-called Quenching and Partitioning (Q&P) is a novel process intended to obtain high strength steels with good ductility to improve fuel economy while promoting passenger safety [3, 4]. With a final microstructure of martensite and retained austenite, Q&P treated steels exhibit an excellent combination of strength and ductility, which allows their use in a new generation of advanced high strength steels (AHSS) for automobiles. The application of Q&P process to a variety of steels results in interesting combinations of mechanical properties that cover the existing gap between TRIP, dual-phase (DP), and martensitic steels [5, 6]. In the Q&P process, the steel is partially or fully austenitized, followed by first rapid cooling by an interrupted quench to a temperature between the martensitic start ( $M_s$ ) and martensite finish ( $M_f$ ) temperatures to form a controlled mixture of martensite and austenite then, in the partitioning step, the steel is isothermally held either at the quenching temperature (one-step) or at higher temperature (two-step) in order to induce the diffusion of carbon from the supersaturated martensite into untransformed austenite, finally the steel is quenched to room temperature and the less stable austenite transforms to martensite, whereas the austenite that is sufficiently carbon enriched stabilizes at room temperature [4, 7-9]. Since Q&P treatment has gained interest for its potential to enhance properties of strength and ductility, some researchers [4, 10-20] have investigated the relationship between properties and microstructures of steels subjected to Q&P heat treatments and showed that the high strength of steels results from martensite laths, while its good ductility is attributed to TRIP-assisted behavior of retained austenite during deformation.

The goal of the present research is to find the best combination of strength and ductility through the microstructure generated after

Q&P heat treatments for the selected CSiMn (TRIP) steel. The partitioning step determines the fraction of retained austenite that can be stable after final quench to room temperature. Therefore, Q&P treatments under different partitioning condition are applied to the investigated steel. It is expected that the presence of certain amounts of retained austenite in combination with a martensitic microstructure could improve the formability of the material without significant strength loss. The ductility and strain hardening are assessed from uniaxial tensile testing, whereas the steel capability to deformation without cracking is evaluated through three-point bending testing.

## 2. Prediction of the optimum quench temperature

Q&P treatment highly depends on the appropriate selection of process parameters and alloy steel. The influence of different Q&P parameters on the structure development and mechanical properties was investigated on a commercially produced TRIP steel sheet with chemical composition of 0.19C-1.84Si-1.68Mn (wt %) in the hot rolled condition with a thickness of 1.6 mm. Flat specimens with dimensions of 7 x 4 x 1.6 mm were machined for dilatometry. A Bähr DIL 805 deformation dilatometer was used to measure the critical temperature points  $A_{c1}$  and  $A_{c3}$ , the results are shown in Table 1. Based on these results, the austenitizing parameters, above  $A_{c3}$ , of 980 °C for 300 seconds were selected for the design of the Q&P treatments. After austenitization, the  $M_s$  and  $M_f$  temperatures were also measured during the quenching of the specimen. A cooling rate of 50 °C/s was applied in order to obtain a fully martensitic microstructure. The experimental values of the  $M_s$  and  $M_f$  temperatures are reported in Table 1.

**Table 1.** Critical temperatures experimentally measured by dilatometry for the studied CSiMn steel.

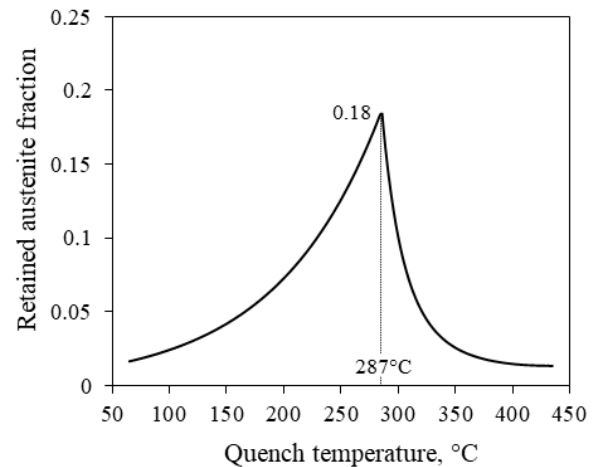
Ac3	Ac1	Ms	M <sub>f</sub>
922 °C	739 °C	389 °C	199 °C

The quench temperature selection methodology developed by Speer [7] was used to predict the “optimum” quench temperature corresponding to the maximum amount of retained austenite that can be stable at room temperature. According to Koistinen and Marburger [21], the predicted fraction of austenite that transforms to martensite  $f_m$  is related to the quenching temperature (QT), as is described in Eq. 1:

$$f_m = 1 - e^{-0.011(M_s - QT)} \quad \text{Eq. 1}$$

The linear formula proposed by Andrews [22] was used to calculate the Ms for input to the Koistinen-Marburger equation. The calculated Ms of 402 °C is in good agreement with the experimental Ms of 389 °C measured by dilatometry (Table 1). The calculations for the prediction of the optimum QT are based upon the nominal chemical composition of the steel grade, full austenitization, and the assumption of ideal carbon partitioning from martensite to austenite where all other competing reactions are suppressed and the amount of retained austenite would be the maximal. The initial QT above Ms was calculated based on the predicted amount of martensite fraction using Eq. 1. Then, Eq.1 was applied again to calculate the amount of final austenite during cooling to room temperature after partitioning step. Figure 1 shows that the QT corresponding to the maximum amount of retained austenite is reached at 287 °C, the estimated fractions of martensite and austenite are 0.82 and 0.18, respectively. The calculated QT corresponds to the retained austenite with a Ms

temperature equal to room temperature after partitioning step. By definition, with the QT of 287 °C all the austenite formed will not transform to martensite after final quench, indicating that the carbon concentration in the retained austenite is high enough to stabilize the austenite at room temperature. For practical application, a QT of 290 °C will be used for subsequent Q&P treatments.

**Figure 1.** Calculated volume fractions of retained austenite as a function of the quenching temperature for the studied CSiMn steel.

### 3. Experimental procedure

Heat treatments series were conducted to evaluate the effect of partitioning step on the microstructure and mechanical properties of the steel, as is shown in Fig. 2. The quench temperature was selected to achieve the maximum retained austenite fraction (section 2) and the variations in the partitioning condition are to optimize the Q&P. All specimens were austenitized at 980 °C for 300s, subsequently quenched at 290 °C, followed by selected partitioning heat treatments. In order to evaluate the effect of the partitioning temperature (PT), partitioning was performed at 290 °C (at QT or one-step), 370 and 440 °C (two-step) under fixed partitioning time of 100 seconds (Fig. 2a). Then, to evaluate the effect of partitioning time (Pt), a PT of 440 °C was

chosen for subsequent heat treatments applying times for 10, 100 and 300s (Fig. 2b). The heat treatments were conducted using salt baths. Final quench at room temperature (RT) was performed in air.

The microstructures were evaluated by light optical microscopy (LOM) and scanning electron microscopy (SEM). The specimens were mounted in bakelite, grinded and polished by standard mechanical methods and

etched with 2 % Nital solution (98 ml ethanol and 2 ml nitric acid). In addition, microstructures were examined by LOM using color etching technique with Klemm reagent for better contrast among phases martensite and retained austenite. Besides, the volume fraction of retained austenite was analyzed by Rietveld analysis using a Bruker D8 advance X-ray diffractometer equipped with a Fe X-ray source. Specimens were electropolished and mounted in bakelite.

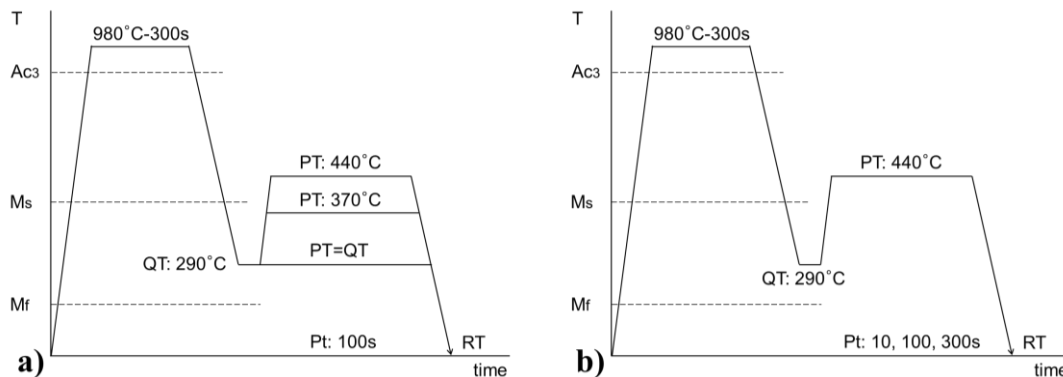


**Figure 2.** Scheme of the Q&P treatments applied to the CSiMn steel to a) evaluate the effect of partitioning temperature (PT) and b) to evaluate the effect of partitioning time (Pt).

Tensile specimens were machined after Q&P treatments according to the geometry indicated in Fig. 3. The uniaxial tensile tests were performed at room temperature in the universal tensile machine Zwick-Z100 according to DIN ISO 6892-1 [23] using a constant cross velocity of 0.5 mm/min. The strain was determined using the optical system to measure the deformation between the two gauge marks. Data of specimens broken outside the gauge length were not considered as part of the analysis. In addition to the engineering stress-strain curves, the strain hardening was also calculated by using the data obtained from the tensile tests.

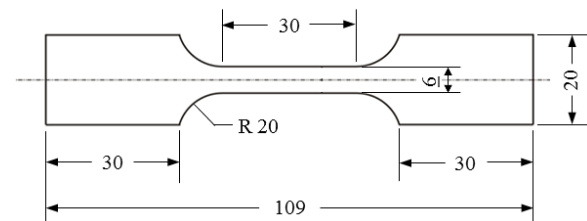


**Figure 3.** Geometry of the tensile specimen. Dimensions are given in mm.

The three-point bending test is a procedure to evaluate the formability of materials to undergo plastic deformation in vending condition. Bending tests were carried out according to DIN EN ISO 7438 [24] on heat treated specimens with dimensions of 60 x 20 x 1.6 mm. Based on the thickness of the specimens, a punch radius of 0.5 mm was used to expose the material to maximum stress. The experiments were conducted with a 5 mm/min punch speed. The bending test was interrupted until the specimen fracture.

The results were plotted in bending force versus bending angle graphs.

## 4. Results and discussion

### 4.1 Tensile properties

The mechanical tensile properties and retained austenite fractions of the studied CSiMn TRIP steel are presented and discussed as follows.

Figure 4 shows the effect of temperature on the tensile properties and the fractions of retained austenite for specimens partitioned at 290 (one-step), 370 and 440 °C for 100 seconds, where retained austenite was determined by X-ray diffraction.

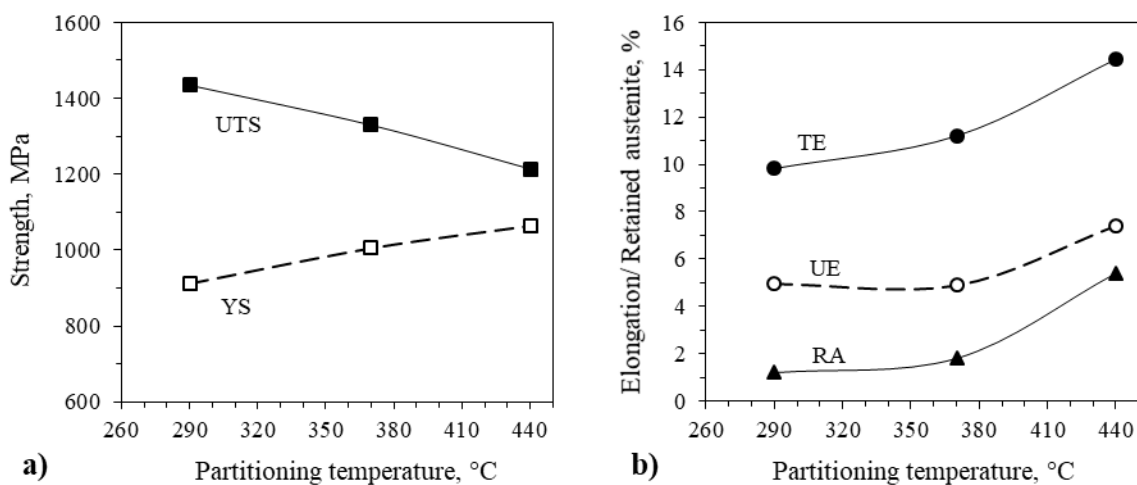
Specimens partitioned at lower temperature show higher tensile strength (Fig. 4a) but also lower elongation (Fig. 4b). The higher strength level obtained after partitioning at 290 °C could be owing to carbon trapping or precipitation in the martensite.

Consistent with the reduced strength (Fig. 4a), the total and uniform elongation are significantly higher for specimens partitioned at 440 °C (Fig. 4b). It is possible that more carbon depletion occurs at higher PT [25],

which could contribute to austenite retention but lower the strength of the martensite. Unlike the tensile strength, the yield strength increases with increasing PT (Fig. 4a).

Figure 4b) also shows that the experimental measured fraction of retained austenite was influenced by the partitioning condition, the volume fraction of retained austenite increases with increasing PT. The highest values of both total and uniform elongation observed after partitioning at 440 °C are consistent with the highest fraction of retained austenite of 5.4 %. This suggests that at 440 °C the TRIP effect is stronger, presumably because larger amounts of retained austenite are stabilized and not decomposed [25]. The lower elongations with partitioning at 290 and 370 °C is related to the small fractions of retained austenite of 1.2 and 1.8 % respectively which have little or no influence on the improvement of the elongation.

The reduced austenite content of the CSiMn steel at PT of 290 and 370 °C can be due to that in the initial stages of partitioning at low temperatures, between 100 and 300 °C, carbon is rather expected to partition into austenite or trapped in dislocations [26].



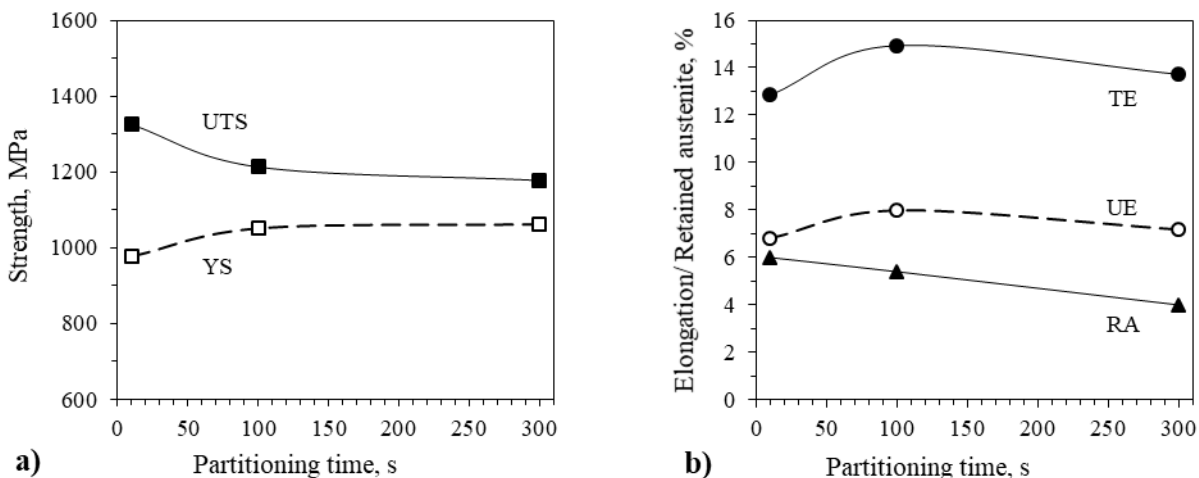
**Figure 4.** a) Tensile properties and b) elongation and retained austenite for specimens partitioned at 290 (1-step), 370 and 440 °C for 100s. UTS: ultimate tensile strength, YS: yield strength, TE: total elongation, UE: uniform elongation, RA: retained austenite.

Figure 5 presents the effect of time on the tensile properties and the content of retained austenite (evaluated by X-ray diffraction) for samples partitioned at 440 °C for 10, 100, and 300s. Figure 5a) shows that the ultimate tensile strength is decreased with increasing Pt, while the yield strength is increased with Pt. Nevertheless, both tensile and yield strength remain almost unchanged after partitioning for 100 and 300 seconds. The highest strength level is obtained for the specimen partitioned for 10 seconds.

Figure 5b) shows that the highest total and uniform elongation are reached after 100 seconds of partitioning with a considerable high tensile strength of 1213 MPa. It is also noticed that the retained austenite gradually decreases with increasing Pt. Nevertheless, the maximum amount of experimentally

measured austenite of 6 % with partitioning at 440 °C for 10 seconds is lower than the maximum amount of predicted austenite of 18 % by the quench temperature methodology (Fig. 1). In this case, the deviation from the predicted results is indicative of incomplete partitioning and formation of bainite or carbide precipitation during the partitioning step [9], which competes with carbon partitioning and lead to a decrease of the volume fraction of retained austenite.

These results could indicate that with partitioning at 440 °C the volume fraction of retained austenite obtained after different Pt is not directly related with the level of elongation. Though, this will be explained in further section 4.5 retained austenite fraction of this work.



**Figure 5.** a) Tensile properties and b) elongation and retained austenite for specimens partitioned at 440 °C for 10, 100 and 300s. UTS: ultimate tensile strength, YS: yield strength, TE: total elongation, UE: uniform elongation, RA: retained austenite.

#### 4.2 Microstructural evaluation

Figure 6 compares the Klemm etched LOM micrographs (on the left) and Nital etched SEM micrographs (on the right) of specimens partitioned for different temperatures and times.

Figures 6a), c), e), g), and i) show the microstructure evaluation by LOM using color etching with Klemm reagent at different partitioning condition. The retained austenite is illustrated in white while martensite is colored in brown and blue. The quantified fractions of austenite for different PT for 100s

are 1.5 % for specimen partitioned at 290 °C (Fig. 6a), 2 % for specimen partitioned at 370 °C (Fig. 6c) and 5 % for specimen partitioned at 440 °C (Fig. 6e). While Figs. 6g) and i) indicate that the retained austenite fraction for specimens partitioned at 440 °C for 10 and 300s are 6 and 4 %, respectively. These fractions of retained austenite are in good agreement with the fractions measured by XRD (Figs. 4b and 5b).

The influence of temperature is evaluated in SEM specimens partitioned at 290 °C (1-step), 370 °C, and 440 °C, illustrated in Figs. 6b), d), and f), respectively. The holding time was 100s for all PT. Specimens present a very fine microstructure consisting of martensite laths with some transition carbides inside. The presence of carbides in specimens partitioned at 370 and 440 °C could be due to the autotempering of the martensite before partitioning [27] (during the transfer from the salt bath for quenching to the salt bath for partitioning). Nevertheless, precipitation during partitioning cannot be excluded since no quantitative measurements of carbides density were conducted. The SEM micrographs also indicate that the martensite structure has a roughening tendency with increasing PT, which can be related to partitioned martensite [28]. In these micrographs, retained austenite is not

distinguished from martensite. Even though, bainite and cementite were not identified by SEM, the presence of transition carbides was observed for all partitioning conditions analyzed. The silicon content of the investigated CSiMn steel can inhibit formation of cementite at high PT but it has poor or no effect in suppressing transition carbide precipitation at low PT [29]. Thereby, due to the small fractions of retained austenite, it can be assumed that stronger precipitation of transition carbides happened with lower PT at 290 and 370 °C.

The effect of time is evaluated with partitioning at 440 °C for 10, 100 and 300s, presented in Figs. 6h), f), and j), respectively. For all specimens, the retained austenite is not observed possibly because it is too fine to be detected by SEM. Cementite was not observed for any of these specimens. Bainite formation was not detected, probably it did not occur since longer Pt is required. Microstructures also show some laths of fresh martensite, which increase with time. This increase in fresh martensite coincides with the decrease in the volume fraction of retained austenite showed in Figs. 6f), h), and j). It is also noticed slightly more carbides formation with partitioning for 300s, which hinder the stabilization of higher fractions of austenite.

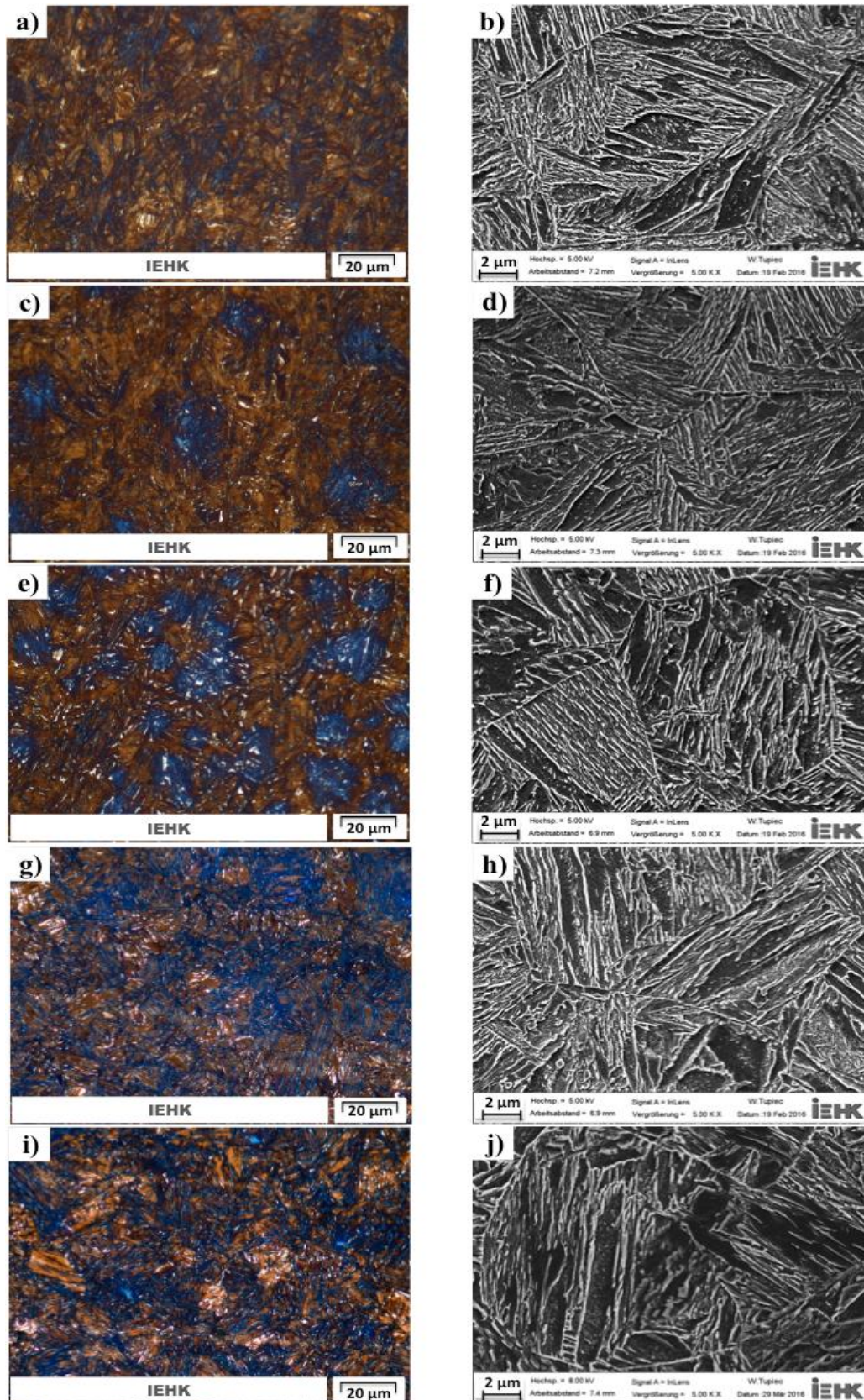


**Figure 6.** Klemm etched LOM micrographs (on the left) and Nital etched SEM micrographs (on the right) for Q&P specimens: a, b) 290 °C-100s, c, d) 370 °C-100s, e, f) 440 °C-100s, g, h) 440 °C-10s, and i, j) 440 °C-300s.

Figure 7 presents the SEM micrographs of the central fracture regions of tested tensile specimens at different PT for 100 seconds. The specimen partitioned at 290 °C (Fig. 7a) shows fine and shallow ductile dimples, it is also observed evidence of cleavage type fracture with a flat faceted appearance. Similar fracture surface is observed in the specimen partitioned at 370 °C (Fig. 7b), which in addition results in several microcracks. Fine and homogeneous dimples caused by void nucleation and coalescence

are clearly visible in specimen partitioned at 440 °C (Fig. 7c), suggesting the ductile nature of the fracture. Cleavage facets are not observed for specimen partitioned at 440 °C indicating smaller or no brittle fracture zones. Thereby, once the cracks initiate, they will propagate more easily throughout specimens partitioned at 290 and 370 °C due to the shallow dimples and primarily cleavage facets resulting in less ductile fractures, which correspond with their respective lower elongation, as showed in Figs. 4b) and 5b).

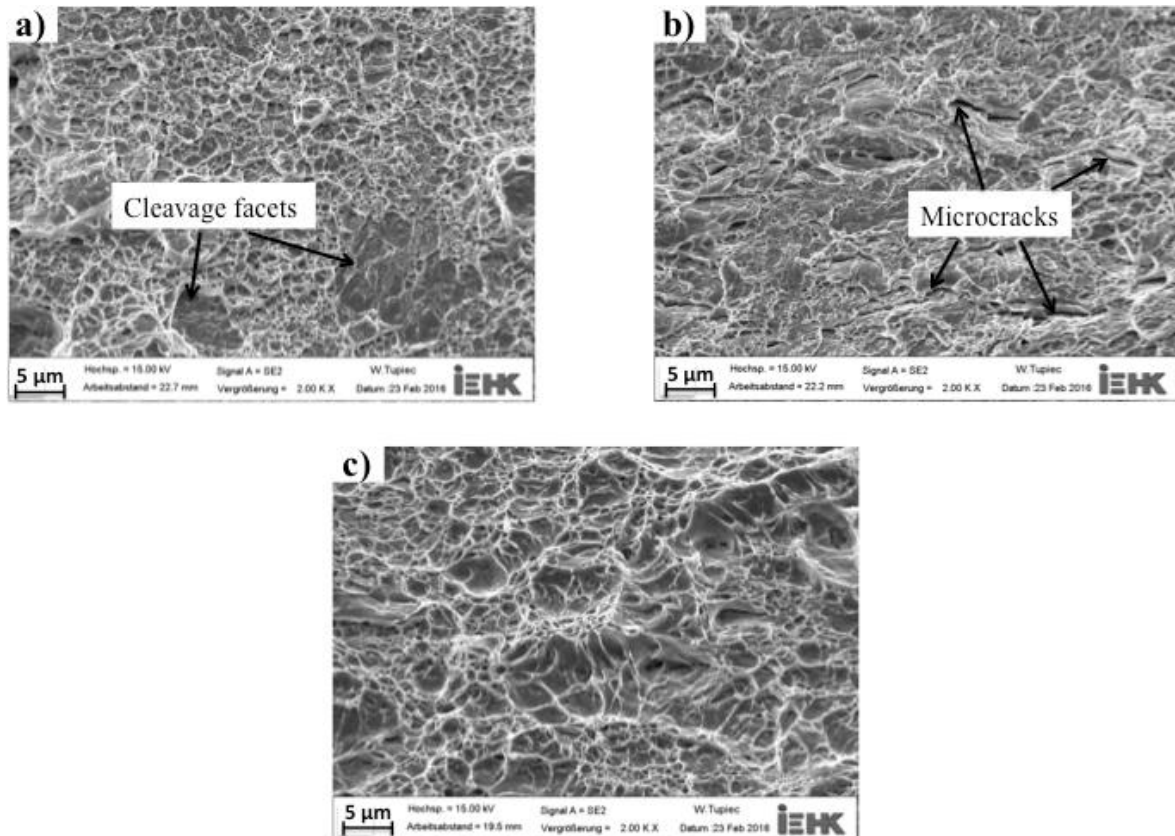


**Figure 7.** Fracture surface of tensile specimens partitioned at: a) 290 (1-step), b) 370 and c) 440 °C for 100s.

#### 4.3 Strain hardening

The strain hardening (or work hardening) is often used as an indication of material formability because it corresponds to the value of uniform elongation in the engineering stress/strain curve. The strain

hardening behavior is investigated based on the Hollomon equation:  $\sigma = K\varepsilon^n$  [30]. Thus, the instantaneous strain hardening exponent can be written as:

$$n = \frac{\partial \ln \sigma}{\partial \ln \varepsilon} = \frac{\ln \sigma_2 - \ln \sigma_1}{\ln \varepsilon_2 - \ln \varepsilon_1} \quad \text{Eq. 2}$$

Where  $\sigma$  is the true stress,  $\varepsilon$  is the true strain and  $n$  is the instantaneous strain hardening exponent.

Figure 8 shows the engineering stress-strain curves and the instantaneous  $n$ -values for specimens partitioned at 290, 370 and 440 °C for 100 seconds. It is noticed that the elongation is significantly increased with increasing PT, indicating a stronger TRIP effect (Fig. 8a).

Figure 8b) indicates that specimens partitioned at lower temperature exhibit much less strain hardening consistent with their

higher strength (Fig 8a). An initial sharp decreasing in instantaneous  $n$ -value curves is observed for all PT up to different strain levels. Then, instantaneous  $n$ -values gradually increase and finally drop again. These variations in instantaneous  $n$ -value are related to the three stages of deformation [31-34]: in the stage I, the  $n$ -value decreases rapidly, the stage II is characterized by a plateau before necking and in the stage III, a second decrease of  $n$ -value is observed. The stage II is considered to be associated with the mechanical stability of retained austenite and the TRIP effect produced by the transformation of retained austenite to martensite [35]. Therefore, the largest plateau observed with partitioning at 440 °C is consistent with the highest content of retained austenite observed in Fig. 4b).

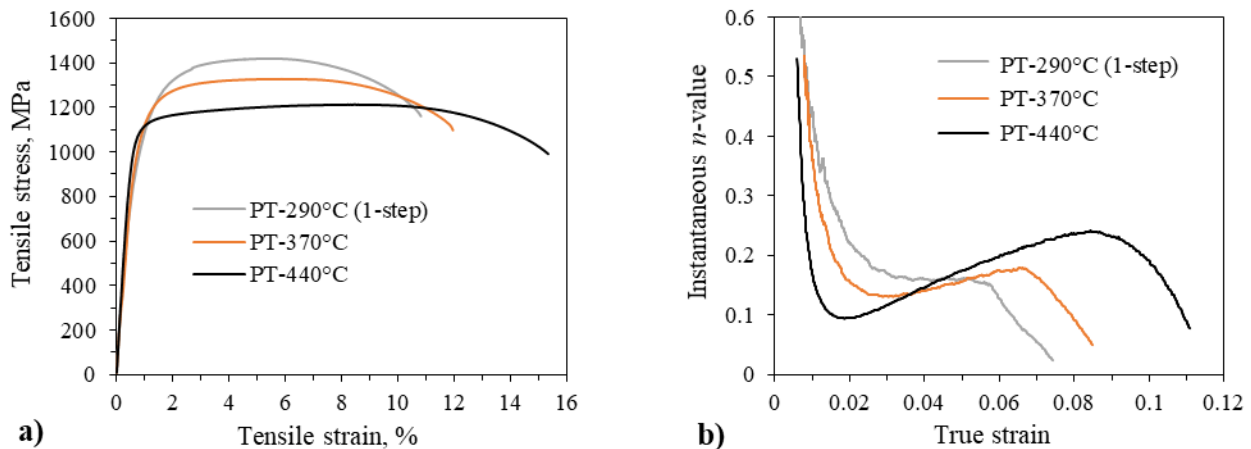


**Figure 8.** Plots of a) engineering stress-strain curves and b) instantaneous  $n$ -value versus true strain for specimens partitioned at 290 (1-step), 370 and 440 °C for 100s.

The engineering stress-strain curves and instantaneous  $n$ -values for specimens partitioned at 440 °C for 10, 100 and 300 seconds are presented in Fig. 9.

Figure 9a) shows that the highest total elongation reached after 100 seconds of partitioning corresponds with the highest  $n$ -values maintained at larger amounts of strain, presented in Fig 9b). The elongation reaches its maximum of 14.9 % with partitioning for

100 seconds resulting also in sustained  $n$ -values at larger strains, where strain hardening is critical for suppressing localization (necking) and failure [36]. A variety of different characteristics such as austenite volume fraction, carbide precipitation, dislocation density, etc. may alter when changing the partitioning conditions [25]. These aspects could have influence on the strain hardening. The three

stages of deformation are also observed for the Pt analyzed in Fig. 9b).

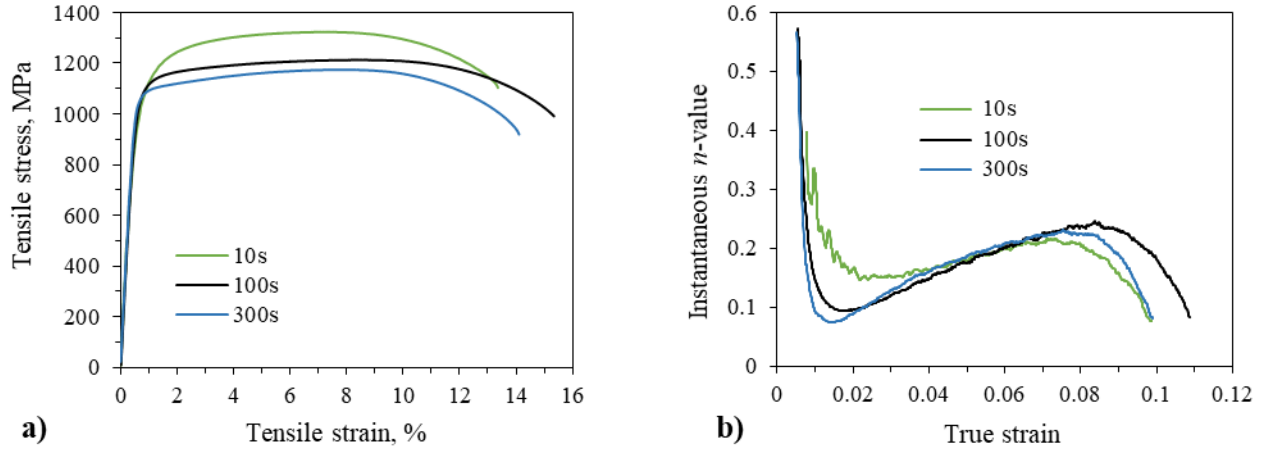


**Figure 9.** Plots of a) engineering stress-strain curves and b) instantaneous  $n$ -value versus true strain for specimens partitioned at 440 °C for 10, 100 and 300s.

#### 4.4 Bendability

Generally, the performance of the parts to resist impact deformation mainly depends on the bending property of the material in conventional stamping [37]. As the failure in the tensile test, the specific failure behaviour of steels in the bending test is of high interest in the context of improvement crash worthiness of safety structural automotive body parts.

The three-point-bending test results for samples partitioned at 290, 370 and 440 °C for 100 seconds are displayed in Fig. 10a). The bendability presents a significant dependence on the PT applied. The bending force decreases with increasing PT, whereas the bending angle increases with increasing PT. Therefore, the bending angle is notably enhanced at partitioning temperature of 440 °C.

Figure 10b) shows that the bending angle at the maximum bending force is increased with increasing PT following similar tendency than the total elongation (data from Fig. 4b) since the highest bending angle at the maximum bending force and the highest elongation are observed at 440 °C of partitioning. It can be assumed that the bendability is strongly correlated with the total elongation of the investigated CSiMn steel for the same Q&P condition. Then, the bending angle could be also influenced by the content of retained austenite and its stability. Nevertheless, a dedicated investigation of the effect of retained austenite on the bendability of the investigated steel should be done. Further investigation concerning the nature of the bending fracture and spring back also needs to be conducted for a complete assessment of the overall material performance.

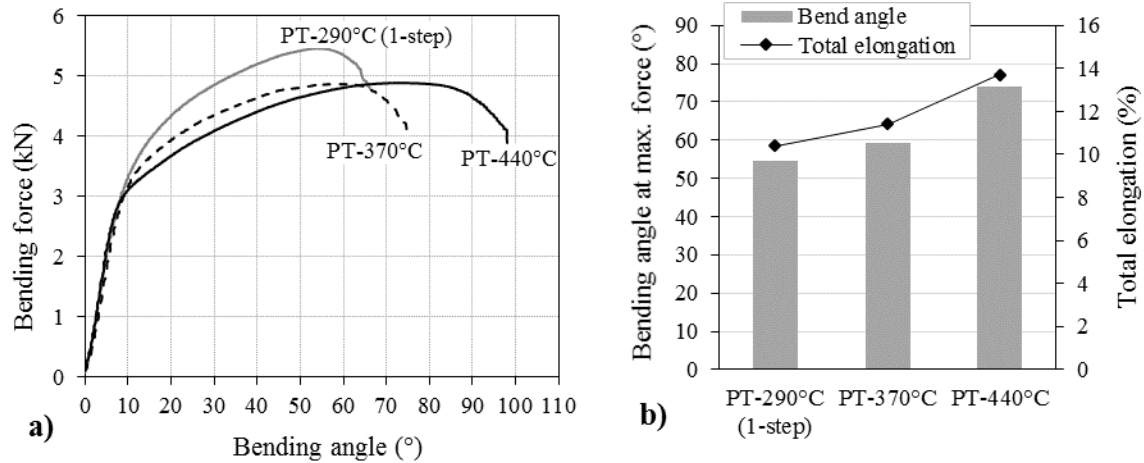


**Figure 10.** a) Bending force/angle curves and b) bending angle at maximum force and total elongation for specimens partitioned at 290 (1-step), 370 and 440 °C for 100s.

#### 4.5 Retained austenite fraction

In this section, the influence of partitioning parameters, time and temperature, on the amount of retained austenite and its stabilization are discussed since an essential purpose of Q&P process is to maintain the stability of retained austenite gained.

Different combinations of microstructural features influence the mechanical properties of the steel as the harder fresh martensite alters the strain distribution between the tempered martensite and austenite. The fractions of these phases and the carbon content of the austenite produced by different heat treatment conditions determine the final mechanical properties. It is known that during the partitioning step the time also plays an important role since it determines the kinetics of carbon diffusion in austenite [38, 39]. In the partitioning process, the average diffusion distance of carbon in the adjacent austenite as a function of time  $t$  can be estimated by Eq. 3 [40]:

$$x_{\gamma}^c = \sqrt{6D_{\gamma}t} \quad \text{Eq. 3}$$

Where  $x_{\gamma}^c$  is the average diffusion distance and  $D_{\gamma}$  is the diffusion coefficient of carbon in austenite that can be expressed as:

$$D_{\gamma} = D_{\gamma 0} \exp(-Q_{\gamma}/RT), \quad \text{Eq. 4}$$

Where  $D_{\gamma 0}$  is a constant [41] ( $D_{\gamma 0} = 0.1 \times 10^{-4} m^2 s^{-1}$ ),  $Q_{\gamma}$  is the activation energy for carbon diffusion [41] ( $Q_{\gamma} = 135.7 kJ/mol$ ),  $R$  is the universal gas constant and  $T$  is the absolute temperature. The diffusion distance of carbon in austenite as a function of time for partitioning at 290 (one-step), 370 and 440 °C is shown in Fig. 11. The partitioning time to stabilize an austenite grain of 1000 nm (1  $\mu m$ ) in diameter based on the average diffusion distance presented in Fig. 11 was calculated to be 64,320 s at 290 °C, 1,740 s at 370 °C and 144 s at 440 °C. Consequently, at 290 and 370 °C very long times are needed for carbon diffusion, stabilization and carbon enrichment of the austenite [38, 42]. This also explains the low fractions of retained austenite ranged between 1 and 2 % with partitioning at 290 and 370 °C for 100 seconds (Fig. 4b). However, prolonged partition time increases the possibility of bainitic transformation and carbide precipitation [42].

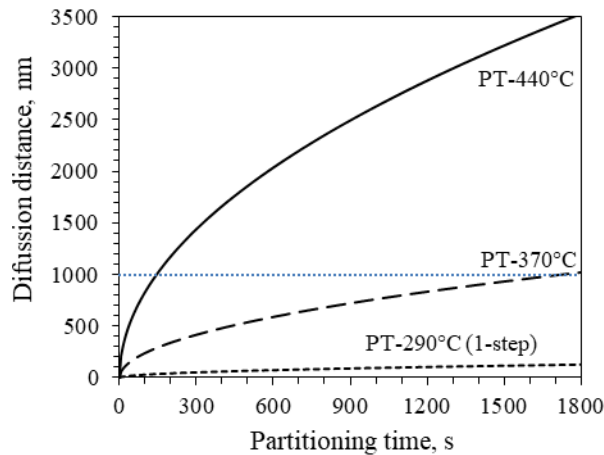


**Figure 11.** Diffusion of carbon in austenite as a function of time for partitioning at 290 (1-step), 370 and 440 °C.

The volume fraction of retained austenite and its stabilization play an important role for the level of enhancement of the elongation, which is mainly controlled by the strain induced transformation behavior of the retained austenite [43]. The mechanism of

elongation improvement is discussed through the mechanical stability and strain-induced transformation behaviour of retained austenite. Therefore, the stability of retained austenite related to strain is evaluated according to the following equation [44]:

$$k = -\ln(f_{\gamma}/f_{\gamma 0})/\varepsilon \quad \text{Eq. 5}$$

where  $k$  is a constant inversely proportional to the stability of austenite being smaller for a very stable austenite,  $f_{\gamma}$  and  $f_{\gamma 0}$  are the volume fractions of retained austenite measured before and after straining, respectively, and  $\varepsilon$  is the uniform true strain. The retained austenite fractions of specimens nearest to the tensile fracture specimen were used as the  $f_{\gamma}$ . Smaller  $k$  values indicate higher stabilization of retained austenite. The  $k$  values obtained are shown in Fig. 12. For better understanding, the previously obtained values of retained austenite and uniform elongation (from Fig. 4b) are also included in Fig. 12.

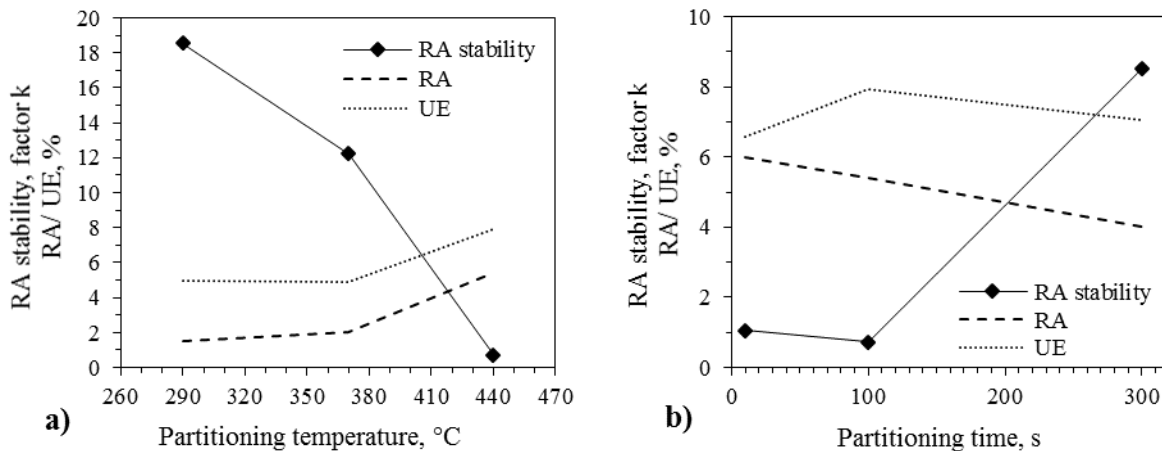


**Figure 12.** Retained austenite stability factor: a) as a function of partitioning temperature (PT) of specimens partitioned for 100s and b) as a function of partitioning time (Pt) for specimens partitioned at 440 °C. Smaller  $k$  values indicate higher stabilization of retained austenite. RA: retained austenite, UE: uniform elongation.

Figure 12a) depicts the stability of retained austenite versus PT of specimens partitioned for 100 seconds. It is noticed that as the PT increases, the mechanical stability of retained

austenite becomes higher. The enhancement of uniform elongation of specimen partitioned at 440 °C is consistent with the higher amount of retained austenite and its

stability. Figure 12b) shows that partitioning at 440 °C contributes to the stabilization of larger fractions of retained austenite for shorter Pt. The highest stability of retained austenite after 100 seconds of partitioning is consistent with the highest value of uniform elongation. Partitioning for 300 seconds results in a large proportion of retained austenite without enough carbon content that cannot be stabilized after the second quenching to room temperature [45], consequently the elongation is decreased. Thereby, the enhanced elongation with partitioning at 440 °C for 100 seconds is explained by a significant TRIP effect due to larger amounts of metastable retained austenite, which gradually transforms into martensite and suppresses a rapid decrease in the strain hardening exponent [46, 47]. Following this observation, the elongation of the Q&P CSiMn steel is mainly controlled by the strain induced transformation behavior of retained austenite [43].

## 5 Conclusions

The current investigation has characterized the mechanical response of the 0.19C-1.84Si-1.68Mn (wt %) TRIP steel undergone Q&P treatments involving variation of the partitioning condition. The studied steel achieved the best combination of tensile strength and total elongation of 1213 MPa and 14.9 % with partitioning at 440 °C for 100 seconds. At this condition, the stability of the retained austenite is the highest indicating a strong TRIP effect which also contributes to the strain hardening. On the other hand, after partitioning at lower temperatures, the small amounts of stable retained austenite due to carbide precipitation produce a weak TRIP effect resulting in lower elongation values.

The outcomes of the three-point bending tests indicate that the bendability is strongly influenced by partitioning temperature. Higher bending angles were obtained with

increasing temperature. Suggesting that the bendability is correlated with the total elongation of the material for the same Q&P conditions applied. This indicates that the bendability could be significantly improved by adjusting the amount of retained austenite through Q&P treatments.

## Acknowledgements

This work was supported by the National Council of Science and Technology (CONACYT) of Mexico and the Institute of Innovation and Transfer of Technology (I<sup>2</sup>T<sup>2</sup>) of Nuevo León.

## References

- [1] M. Merklein, J. Lechler, and M. Geiger: *Ann. CIRP. - Manuf. Technol.*, 2006, vol. 55, pp. 229-232.
- [2] T. Altan and A.E. Tekkaya: *Sheet metal forming: Process and applications*, ASM International, OH, USA, 2012.
- [3] D.K. Matlock, J.G. Speer, E. De Moor, and P.J. Gibbs: *Jestech*, 2012, vol. 15, pp. 1-12.
- [4] J.G. Speer, F.C. Rizzo, D.K. Matlock, and D.V. Edmonds: *Mater. Res.*, 2005, vol. 8, pp. 417-423.
- [5] J.G. Speer, D.V. Edmonds, F.C. Rizzo, and D.K. Matlock: *Curr. Opin. Solid State Mater. Sci.*, 2004, vol. 8, pp. 219-237.
- [6] D.V. Edmonds, K. He, F.C. Rizzo, A.M.S. Clarke, D.K. Matlock, and J.G. Speer: proceedings of the 1<sup>st</sup> International Conference on Super High Strength Steels, Rome, 2005, pp. 1–20.
- [7] J. G. Speer, D.K. Matlock, B.C. De Cooman, and J.G. Schroth: *Acta Mater.*, 2003, vol. 51, pp. 2611–2622.

- [8] Y. Toji, H. Matsuda, M. Herbig, P-P. Choi, and D. Raabe: *Acta Mater.*, 2014, vol. 65, pp. 215-228.
- [9] A.J. Clarke, J.G. Speer, M.K. Miller, R.E. Hackenberg, D.V. Edmonds, D.K. Matlock, F.C. Rizzo, K.D. Clarke, and E. De Moor: *Acta Mater.*, 2008, vol. 56, pp. 16–22.
- [10] D.K. Matlock and J.G. Speer: proceedings of the Third International Conference on Structural Steels, Seoul, 2006, pp. 774–781.
- [11] D.V. Edmonds, K. He, M.K. Miller, F.C. Rizzo, A. Clarke, and D.K. Matlock: Fifth International Conference on Processing and Manufacturing of Advanced Materials, Vancouver, 2006, pp. 4819–4825. <sup>[1]</sup><sub>SEP</sub>
- [12] K. He, D.V. Edmonds, J.G. Speer, D.K. Matlock, and F.C. Rizzo: EMC 2008 14th European <sup>[1]</sup><sub>SEP</sub> Microscopy Congress, Aachen, 2008, pp. 429–430.
- [13] S.S. Nayak, R. Anumolu, R.D.K. Misra, K.H. Kim, and D.L. Lee: *Mater. Sci. Eng. A*, 2008, vol. 498, pp. 442–456.
- [14] M.J. Santofimia, L. Zhao, R. Petrov, and J. Sietsma: *Mater. Charact.*, 2008, vol. 59, pp.1758-1764.
- [15] C.Y. Wang, J. Shi, W.Q. Cao, and H. Dong: *Mater. Sci. Eng. A*, 2010, vol. 527, pp. 3442–3449.
- [16] J.G. Speer, E. De Moor, K.O. Findley, D.K. Matlock, B.C. De Cooman, and D.V. Edmonds: *Metall. Mater. Trans. A*, 2011, vol. 42A, pp. 3591–3601.
- [17] G. Thomas, J. Speer, D. Matlock, and J. Michael: *Microsc. Microanal.*, 2011, vol. 17, pp. 368-373.
- [18] M.J. Santofimia, L. Zhao, and J. Sietsma: *Scr. Mater.*, 2008, vol. 59, pp.159–162.
- [19] M.J. Santofimia, J.G. Speer, A.J. Clarke, L. Zhao, and J. Sietsma: *Acta Mater.*, 2009, vol. 57, pp. 4548–4557.
- [20] Y. Takahama, M.J. Santofimia, M.G. Mecozzi, L. Zhao, and J. Sietsma: *Acta Mater.*, 2012, vol. 60, pp. 2916–2926.
- [21] D.P. Koistinen and R.E. Marburger: *Acta Metall.*, 1959, vol. 7, pp. 59-60.
- [22] K.W. Andrews: *Iron and Steel Institute Journal* 203, 1965 part 7, pp. 721–727.
- [23] ISO 6892-1:2009. Metallic materials - Tensile testing - Part 1: Method of test at room temperature; German version EN ISO 6892-1:2009.
- [24] ISO 7438:2005. Metallic materials - Bend test, 2005.
- [25] E. De Moor, S. Lacroix, A.J. Clarke, J. Penning, and J.G. Speer: *Metall. Mater. Trans.*, 2008, vol. 39, pp. 2586-2595.
- [26] F. Tariq and R.A. Baloch: *J. Mater. Eng. Perform.*, 2014, vol. 23, pp. 1726-1739.
- [27] E. Paravicini, M.J. Santofimia, L. Zhao, J. Sietsma, and E. Anelli: *Mater. Sci. Eng. A*, 2013, vol. 559, pp. 486-495.
- [28] A. Arlazarov, O. Bouaziz, J.P. Masse, and F. Kegel: *Mater. Sci. Eng. A*, 2015, vol. 620, pp. 293-300.
- [29] D.V. Edmonds, K. He, F.C. Rizzo, B.C. De Cooman, D.K. Matlock, and J.G. Speer: *Mater. Sci. Eng.: A*, 2006, vols. 438-440, pp. 25-34.
- [30] J.H. Hollomon: *Trans. AIME*; 1945, vol. 162, pp. 268-290.
- [31] D.B. Santos, R. Barbosa, P.P.d. Oliveira, and E.V. Pereloma: *ISIJ Int.*, 2009, vol. 49, pp. 1592-1600.
- [32] I.B. Timokhina, P.D. Hodgson, and E.V. Pereloma: *Metall. Mater. Trans. A*, 2003, vol. 34, pp. 1599-1609.

- [33] I.B. Timokhina, P.D. Hodgson, and E.V. Pereloma: *Metall. Mater. Trans. A*, 2004, vol. 35, pp. 2331–2341.
- [34] J. Shi, X. Sun, M. Wang, W. Hui, H. Dong, and W. Cao: *Scripta Mater.*, 2010, vol. 63, pp. 815–818.
- [35] S. Zhou, K. Zhang, Y. Wang, J.F. Gu, and Y.H. Rong: *Metall. Mater. Trans. A*, 2012, vol. 43, pp. 1026-1034.
- [36] J. Chiang, B. Lawrence, J.D. Boyd, and A.K. Pilkey: *Mater. Sci. Eng. A*, 2011, vol. 528, pp. 4516-4521.
- [37] R. Ge, Y.J. Bi and H.L. Wei: proceedings of the *2nd International Conference on Advanced High Strength Steel and Press Hardening (ICHSU2015)*, Changsha, China, 2015, pp. 52-56.
- [38] D. De Knijf, E. P. Da Silva, C. Föjer, and R. Petrov: *Mat. Sci. Technol.*, 2015 vol. 31, pp. 817-828.
- [39] H. Y. Li, X. W. Lu, X. C. Wu, Y. A. Min, and X. J. Jin: *Mater. Sci. Eng.: A*, 2010, vol. 527, pp. 6255–6259.
- [40] K. F. Kelton, A. L. Greer, and C. V. Thompson: *J. Chem. Phys.*, 1983, vol. 79, pp. 6261-6276.
- [41] T. Gladman: *The physical metallurgy of microalloyed steels*, Institute of Materials, Cambridge, London, 1997.
- [42] S. Santigopal, D. Sourav, C. Debalay, S. Indradev, B. S. Shiv, and H. Arunansu: *Metall. Mater. Trans. A*, 2013, vol. 44, pp. 5653-5664.
- [43] K. Sugimoto, N. Usui, M. Kobayashi, and S. Hashimoto: *ISIJ Int.*, 1992, vol. 32, pp. 1311–1318.
- [44] K. Sugimoto, M. Kobayashi, and S. Hashimoto: *Metall. Mater. Trans. A*, 1992, vol. 23, pp. 3085-3091.
- [45] N. Zhong, Q. Wu, Y. Yin, and X. Wang: *Steel Research Int.*, 2015, vol. 86, pp. 252-256.
- [46] H. Yin, A. Zhao, Z. Zhao, X. Li, S. Li, H. Hu, and W. Xia: *Int. J. Miner. Metall. Mater.*, 2015, vol. 22, pp. 262-271.
- [47] E. De Moor, C. Föjer, A.J. Clarke, J. Penning, and J.G. Speer: proceedings of the *Conference on New Developments on Metallurgy and Applications of High-Strength Steels, Minerals, Metals & Materials Soc.*, Buenos Aires, 2008, vols. 1 and 2, pp. 721-729.